Communications in Physics, Vol. 33, No. 4 (2023), pp. 355-368
DOI: https://doi.org/10.15625/0868-3166/19043

$\mu - e$ conversion in a model of electroweak scale right-handed neutrino mass

D. N. Dinh[†], **D. T. Man and N. T. Nhuan**

Institute of Physics, Vietnam Academy of Science and Technology,
10 Dao Tan, Ba Dinh, Hanoi 11108, Vietnam

E-mail: [†]dndinh@iop.vast.vn

Received 1 October 2023
Accepted for publication 10 November 2023
Published 8 December 2023

Abstract. *We perform a detailed analysis of the $\mu - e$ conversion within an extended version of the standard model (SM) with mirror symmetry and low energy of the electroweak scale of the type I seesaw neutrino mass generation. After a brief introduction to the model, we derive the $\mu - e$ conversing ratio at one-loop approximation, in which the running inside are W gauge boson or singly charged scalars accompanying with neutrinos, and neutral scalars with new leptons. We focus, mainly, on predictions of observable possibilities and constraints set on relevant couplings from the $\mu - e$ conversion in nuclei.*

Keywords: $\mu - e$ conversion in nuclei, lepton flavor violation process, elementary particle physics, physics beyond the SM.

Classification numbers: elementary particle physics, high energy physics.

1. Introduction

In this research, we work on a class of extended versions of the SM accommodated with the massive neutrinos, which acquire their masses at low energy of the electroweak scale [1]. To achieve this, a new fermion mirror sector is added to the SM by introducing a corresponding mirror partner for each SM fermion with the same quantum numbers but opposite chirality. Right-handed neutrinos, which are the left-handed mirror partners, accompany with the SM neutrinos to operate the type I see-saw mechanism properly functioning [2–5]. This mass generation mechanism is shown to be able to work at the electroweak scale, in contrast to the canonical type I see-saw, which operates at ultra-high energy level.

The phenomenology of $\mu - e$ conversion will be considered in the scenario of a specific version, which was introduced after the 125 GeV SM-like Higgs scalar discovery [6, 7]. By introducing two Higgs doublets, instead of only one in the original versions, two neutral candidates are shown to have signals in agreement with ATLAS and CMS results [7]. Besides, the model has also proved to still have a large range of available parameter space after being constrained by the electroweak precision data [8]. Recently, phenomenology of some lepton flavor violation (LFV) processes has been performed to give observable predictions and set more constraints on the parameter space. At earlier stage, researchers considered only the contribution of the light neutral scalar [6, 9–11]. Subsequently, the contributions of other new heavy particles, including the neutral and singly charged scalars, have also been taken into account [12, 13].

The $\mu - e$ conversion is a hypothetical process in which a muon, after being captured by a nucleus, converts into an electron without emitting any neutrino. The process can occur only in some extended versions of the SM with lepton flavor violations. Therefore it is considered as an important channel in identifying new physics beyond the SM. The present best upper limits of the $\mu - e$ conversion ratios are: $\mathrm{CR}(\mu\mathrm{Ti} \to e\mathrm{Ti}) < 4.3 \times 10^{-12}$ and $\mathrm{CR}(\mu\mathrm{Au} \to e\mathrm{Au}) < 7.0 \times 10^{-13}$ at 90% confidence level by the SINDRUM-II [14, 15]. The future experimental sensitivity for Ti nuclei is expected to be $\mathrm{CR}(\mu\mathrm{Ti} \to e\mathrm{Ti}) \sim 10^{-18}$ [16]. While the designed sensitivities of Mu2e and COMET using Al nuclei are about 10^{-17} [17, 18].

In this research, we will examine the phenomenology of $\mu - e$ conversion in the upgraded version that was introduced after the discovery of the 125 GeV SM-like scalar. In addition to the light scalar, we will also consider contributions from other heavy scalars that have not been previously taken into account. The contents are arranged as follows: Sect. 1 is for introduction. In Sect. 2 we briefly introduce the model and involved LFV vertices. In Sect. 3, the derivation and numerical analysis of the conversion rate are detailedly performed. Finally, Sect. 4 is for conclusions and discussions.

2. A review of the model

2.1. The model content

The model of interest in this research is an extended version of the SM, which is constructed based on the symmetric group $SU(2) \times U(1)_Y \times Z_{SM}^4 \times Z_{MF}^4$, in which $SU(2) \times U(1)_Y$ is the gauge group, and $Z_{SM}^4 \times Z_{MF}^4$ is a discrete global symmetry. The field contents and their transformations under the above symmetry are detailedly shown in Table 1. Discrete symmetry $Z_{SM}^4 \times Z_{MF}^4$ are introduced to prevent some unexpected interactions. Transformations of a given field Ψ with $(\omega_a^\alpha, \omega_b^\beta)$ under $Z_{SM}^4 \times Z_{MF}^4$ are defined as $\Psi \to \omega_a^\alpha \Psi \omega_b^\beta$, where α, β are integer numbers within [0,3] and $\omega_a^4 = \omega_b^4 = 1$.

Note that accompanying with a given SM fermion is a particle, called as mirror partner, with the same quantum number but opposite chirality. The right-handed neutrinos, which naturally appear as mirror partners of those corresponding left-handed ones, are not $SU(2) \times U(1)_Y$ singlets; therefore they are non-sterile and take part in the weak interaction. Apparently, discrete symmetry $Z_{SM}^4 \times Z_{MF}^4$ defined in the earlier part only allows Φ_2 to couple to SM fermions, while Φ_{2M} will

Table 1. Model's field contents and their transformations under gauge and global discrete symmetries, here ω_a, ω_b respectively characterize for Z^4_{SM} and Z^4_{MF} transformations, where ω_a^4=$\omega_b^4 = 1$.

Multiplets	$SU(2)\times U(1)_Y$	Z^4_{SM}	Z^4_{MF}
$\ell_L = (\nu_L,\, e_L)^T$, $q_L = (u_L, d_L)^T$	$(2,-1)$, $(2,1/3)$	ω_a^3	1
$\ell_R^M = (\nu_R,\, e_R^M)^T$, $q_R^M = (u_R^M,\, d_R^M)^T$	$(2,-1)$, $(2,1/3)$	1	ω_b^3
e_R, u_R, d_R	$(1,-2)$, $(1,4/3)$, $(1,-2/3)$	ω_a	1
e_L^M, u_L^M, d_L^M	$(1,-2)$, $(1,4/3)$, $(1,-2/3)$	1	ω_b
$\Phi_2 = (\phi_2^+, \phi_2^0)$	(2,1)	ω_a^2	1
$\Phi_{2M} = (\phi_{2M}^+, \phi_{2M}^0)$	(2,1)	1	ω_b^2
$\chi = \left(\chi^{++}, \chi^+, \chi^0\right)$	(3,2)	1	ω_b^2
$\xi = \left(\xi^+, \xi^0, \xi^-\right)$	(3,0)	1	1
ϕ_S	(1,0)	ω_a^3	ω_b

couple to the mirror partners. The singlet ϕ_S transforms nontrivially under both Z^4_{SM} and Z^4_{MF} will couple to a normal and a mirror fields. Detailed expressions of the Yukawa couplings are:

$$\mathscr{L}_Y^\ell = g_\ell \bar{\ell}_L \Phi_2 e_R + g_\ell^M \bar{\ell}_R^M \Phi_{2M} e_L^M + g_{\ell s} \bar{\ell}_L \phi_s \ell_R^M + g'_{\ell s} \bar{e}_L^M \phi_s e_R + h.c., \tag{1}$$

$$\begin{aligned}\mathscr{L}_Y^q \;=\;& g_u \bar{q}_L \tilde{\Phi}_2 u_R + g_u^M \bar{q}_R^M \tilde{\Phi}_{2M} u_L^M + g_d \bar{q}_L \Phi_2 d_R + g_d^M \bar{q}_R^M \Phi_{2M} d_L^M \\ &+ g_{qs} \bar{q}_L \phi_s q_R^M + g'_{us} \bar{u}_L^M \phi_s u_R + g'_{ds} \bar{d}_L^M \phi_s d_R + h.c.,\end{aligned} \tag{2}$$

$$\mathscr{L}_{\nu_R} = g_M \left(l_R^{M,T}\, \sigma_2\right) (i\tau_2 \tilde{\chi})\, l_R^M\,, \tag{3}$$

where σ_2 and τ_2 are both the second Pauli matrix, $\tilde{\Phi}_2 = i\sigma_2 \Phi_2^*$, $\tilde{\Phi}_{2M} = i\sigma_2 \Phi_{2M}^*$, and $\tilde{\chi}$ is 2 by 2 matrix form of the complex Higgs triplet with $Y = 2$

$$\tilde{\chi} = \begin{pmatrix} \frac{1}{\sqrt{2}}\chi^+ & \chi^{++} \\ \chi^0 & -\frac{1}{\sqrt{2}}\chi^+ \end{pmatrix}. \tag{4}$$

In eq. (3), two different notations are used for the second Pauli matrix to identify that σ_2 acts on the space of two-component Weyl spinors, while τ_2 acts on the space of $SU(2)$ isospin. We expect to have Hermetic charged fermion mass matrices, which simply implies $g'_{\ell s} = g_{\ell s}^\dagger$, $g'_{us} = g_{us}^\dagger$ and $g'_{ds} = g_{ds}^\dagger$, respectively. Note that discussion on the quark sector will not be performed in this letter, because it does not involve in the phenomenology of physical quantity under consideration of this research.

2.2. *Symmetry breaking and mass generations*

Before carry on discussion on the mechanisms of symmetry breaking and mass generation, let us denote the vacuum expectation values (VEV) of relevant Higsgs multiplets as follows: $\langle \Phi_2 \rangle = (0, v_2/\sqrt{2})^T$, $\langle \Phi_{2M} \rangle = (0, v_{2M}/\sqrt{2})^T$, $\langle \chi^0 \rangle = v_M$, and $\langle \phi_S \rangle = v_S$. From eq. (1), charged lepton mass matrix is easily obtained as:

$$M_\ell = \begin{pmatrix} m_\ell & m_\ell^D \\ (m_\ell^D)^\dagger & m_{\ell M} \end{pmatrix}, \tag{5}$$

where $m_\nu^D = m_\ell^D = g_{\ell s} v_S$, $m_\ell = g_\ell v_2/\sqrt{2}$, and $m_{\ell M} = g_\ell^M v_{2M}/\sqrt{2}$. Based on the current experimental status of searching new fermions beyond the standard model, we reasonably assume that $m_{\ell M} \gg m_\ell$ and $m_{\ell M}, m_\ell \gg m_\ell^D$. The assumption allows us to approximately block-diagonalize M_ℓ, the final result arrives at:

$$\tilde{m}_\ell = m_\ell - \frac{(m_\ell^D)^2}{m_{\ell M} - m_\ell} \approx m_\ell,\ \tilde{m}_{\ell M} = m_{\ell M} + \frac{(m_{\ell M}^D)^2}{m_{\ell M} - m_\ell} \approx m_{\ell M}, \tag{6}$$

$$\begin{pmatrix} \ell_{L(R)} \\ \ell_{L(R)}^M \end{pmatrix} = \begin{pmatrix} U_{\ell L(R)} & -R_\ell U_{\ell L(R)}^M \\ R_\ell^\dagger U_{\ell L(R)} & U_{\ell L(R)}^M \end{pmatrix} \begin{pmatrix} \ell'_{L(R)} \\ \ell_{L(R)}^{M'} \end{pmatrix}, \tag{7}$$

where $\ell'_{L(R)}$, $\ell_{L(R)}^{M'}$ are respectively the normal and mirror charged leptons in the mass basis; $R_\ell \approx \frac{m_\ell^D}{m_{\ell M}} \ll 1$, and $\tilde{m}_\ell = U_{\ell L} m_\ell^d U_{\ell R}^\dagger$, $\tilde{m}_{\ell M} = U_{\ell L}^M m_{\ell M}^d U_{\ell R}^{M\dagger}$, in which m_ℓ^d and $m_{\ell M}^d$ are diagonal matrices.

Similarly, neutral leptons achieve their masses through a matrix of canonical form of the type-I see-saw mechanism

$$M_\nu = \begin{pmatrix} 0 & m_\nu^D \\ (m_\nu^D)^T & M_R \end{pmatrix}, \tag{8}$$

where $M_R = g_M v_M$. Approximately block-diagonalizing (8), while keeping in mind that $M_R \gg m_\nu^D$, the result reads

$$\tilde{m}_\nu \approx -\frac{(m_\nu^D)^2}{M_R} = -\frac{(g_{\ell s} v_S)^2}{g_M v_M},\ \tilde{m}_{\nu R} \approx M_R. \tag{9}$$

$$\begin{pmatrix} \nu_L \\ (\nu_R)^c \end{pmatrix} = \begin{pmatrix} U_\nu & -R_\nu U_\nu^M \\ R_\nu^\dagger U_\nu & U_\nu^M \end{pmatrix} \begin{pmatrix} \chi_L \\ \chi_L^M \end{pmatrix}. \tag{10}$$

Here, $R_\nu \approx \frac{m_\nu^D}{M_R}$ is the ratio of the neutrino Dirac and Majorana mass matrices; U_ν and U_ν^M are transformation matrices to diagonalized $\tilde{m}_\nu$ and $\tilde{m}_{\nu R}$, respectively. Although the light neutrino mass matrix $\tilde{m}_\nu$ defined in (9) is experimentally constrained to be at sub-eV order, M_R could be relevant as low as the electroweak scale. For instance, $(g_{\ell s}^2/g_M) \sim O(1)$ and $v_S \sim O(10^5\ eV)$.

We know that when triplets are introduced into the model, the tree-level result $\rho = M_W^2/M_Z^2 \cos^2\theta_W = 1$ might be spoiled out. However, it is proved in [19] that, if the Higgs potential has global $SU(2)_L \otimes SU(2)_R$ symmetry and Higgs alignments are arranged in a way such that a custodial $SU(2)$ symmetry is preserved after the symmetry broken then $\rho = 1$. For the reason, the triplets are arranged to transform as $(3,3)$ and the two doublets as $(2,2)$ under the global symmetry:

$$\chi = \begin{pmatrix} \chi^0 & \xi^+ & \chi^{++} \\ \chi^- & \xi^0 & \chi^+ \\ \chi^{--} & \xi^- & \chi^{0*} \end{pmatrix},\ \Phi_2 = \begin{pmatrix} \phi_2^{0,*} & \phi_2^+ \\ \phi_2^- & \phi_2^0 \end{pmatrix},\ \Phi_{2M} = \begin{pmatrix} \phi_{2M}^{0,*} & \phi_{2M}^+ \\ \phi_{2M}^- & \phi_{2M}^0 \end{pmatrix}. \tag{11}$$

The corresponding vacuum expectation values are:

$$\langle\chi\rangle = \begin{pmatrix} v_M & 0 & 0 \\ 0 & v_M & 0 \\ 0 & 0 & v_M \end{pmatrix},\ \langle\Phi_2\rangle = \begin{pmatrix} \frac{v_2}{\sqrt{2}} & 0 \\ 0 & \frac{v_2}{\sqrt{2}} \end{pmatrix},\ \langle\Phi_{2M}\rangle = \begin{pmatrix} \frac{v_{2M}}{\sqrt{2}} & 0 \\ 0 & \frac{v_{2M}}{\sqrt{2}} \end{pmatrix}. \tag{12}$$

Vacuum expectation values of the real components of Φ_2, Φ_{2M} and χ satisfy the conditions

$$v_2^2 + v_{2M}^2 + 8\,v_M^2 = v^2\,, \tag{13}$$

where $v \approx 246\ GeV$. For convenience in further discussions, the following notations are used:

$$s_2 = \frac{v_2}{v};\ s_{2M} = \frac{v_{2M}}{v};\ s_M = \frac{2\sqrt{2}\,v_M}{v}\,. \tag{14}$$

Next, we discuss the physical scalars, which are generated from the seventeen degrees of freedom of the two Higgs triplets (one real and one complex) and two Higgs doublets after three of them are absorbed to give masses to W's and Z. Those that are mass-degenerate are elements of the same multiplets of the global custodial symmetry. Careful consideration shows that there are a five-plet (quintet) $(H_5^{\pm\pm}, H_5^{\pm}, H_5^0)$, two triplets $(H_3^{\pm}, H_3^0)$, $(H_{3M}^{\pm}, H_{3M}^0)$ and three singlets H_1^0, H_{1M}^0, $H_1^{0\prime}$. Three singlets H_1^0, H_{1M}^0, $H_1^{0\prime}$ are not physical states, in general, they are linear combinations of mass eigenstates $(\tilde{H}_1^0, \tilde{H}_2^0, \tilde{H}_3^0)$ as $H_1^0 = \sum_i^3 \alpha_i \tilde{H}_i$, $H_{1M}^0 = \sum_i^3 \alpha_i^M \tilde{H}_i$, where $\sum_i^3 |\alpha_i|^2 = 1$ and $\sum_i^3 |\alpha_i^M|^2 = 1$. Note that one of the three neutral mass states above is the SM-like Higgs scalar discovered by LHC [7]. Finally, the degree of freedom of the light Higgs ϕ_S is a singlet scalar, denoted as ϕ_s^0, after the mass generation mechanism.

2.3. The LFV vertices

In this under consideration model, the field content is enlarged with mirror fermions, which are not $SU(2)_L$ singlet and thus participate in the weak interactions. Consequently, the LFV interactions can occur at tree-level. Their expressions in the mass basis are detailed in Table 2 and equations from (15) to (20) [12, 13]. To obtain the results, we have dropped terms that are subleading of the second order of $R_{\nu(\ell)}$ and higher and assumed that the charged lepton and mirror charged lepton mixing matrices are real and $U_{\ell L} = U_{\ell R} = U_\ell$, $U_{\ell L}^M = U_{\ell R}^M = U_\ell^M$ for more simplicity in further discussions.

Table 2. Lepton flavor violation vertices that contribute to the process of $\mu \to e$ conversion.

Vertices	Couplings
$(\bar{e}'_L \gamma^\mu \chi_L) W_\mu^-$	$-i\frac{g}{\sqrt{2}} U_{W_\mu}^L = -i\frac{g}{\sqrt{2}} U_{PMNS}$
$(\bar{e}'_L \gamma^\mu \chi_L^M) W_\mu^-$	$-i\frac{g}{\sqrt{2}} U_{W_\mu}^{ML} = i\frac{g}{\sqrt{2}} \tilde{R}_\nu \left(U_{PMNS}^M\right)^*$
$(\bar{e}'_R \gamma^\mu \chi_L^c) W_\mu^-$	$-i\frac{g}{\sqrt{2}} U_{W_\mu}^R = -i\frac{g}{\sqrt{2}} \tilde{R}_\nu^T \left(U_{PMNS}\right)^*$
$\bar{e}'_R \chi_L H_3^-$	$-i\frac{g}{2} Y_{H_3^-}^L = -i\frac{g\ s_M}{2M_W c_M} m_\ell^d U_{PMNS}$
$\bar{e}'_R \chi_L^M H_3^-$	$-i\frac{g}{2} Y_{H_3^-}^{ML} = i\frac{g\ s_M}{2M_W c_M} m_\ell^d \tilde{R}_\nu \left(U_{PMNS}^M\right)^*$
$\bar{e}'_L \chi_L^{Mc} H_3^-$	$-i\frac{g}{2} Y_{H_3^-}^{MR} = -i\frac{g\ s_M}{2M_W c_M} \tilde{R}_\ell m_{\ell M}^d U_{PMNS}^M$
$\bar{e}'_R \chi_L H_{3M}^-$	$-i\frac{g}{2} Y_{H_{3M}^-}^L = -i\frac{g\ s_{2M}}{2M_W s_2 c_M} m_\ell^d U_{PMNS}$
$\bar{e}'_R \chi_L^M H_{3M}^-$	$-i\frac{g}{2} Y_{H_{3M}^-}^{ML} = i\frac{g\ s_{2M}}{2M_W s_2 c_M} m_\ell^d \tilde{R}_\nu \left(U_{PMNS}^M\right)^*$
$\bar{e}'_L \chi_L^{Mc} H_{3M}^-$	$-i\frac{g}{2} Y_{H_{3M}^-}^{MR} = -i\frac{g\ s_M}{2M_W s_{2M} c_M} \tilde{R}_\ell m_{\ell M}^d U_{PMNS}^M$
$\bar{e}'_R e_L^{M\prime} \phi_s^0$	$-i\frac{g}{2} Y_{\phi_s^0}^{ML} = -iU_{\ell R}^\dagger g_{\ell s} U_{\ell L}^M = -i\tilde{g}_{\ell s}$
$\bar{e}'_L e_R^{M\prime} \phi_s^0$	$-i\frac{g}{2} Y_{\phi_s^0}^{MR} = -i\ U_{\ell L}^\dagger g_{\ell s} U_{\ell R}^M = -i\tilde{g}_{\ell s}$

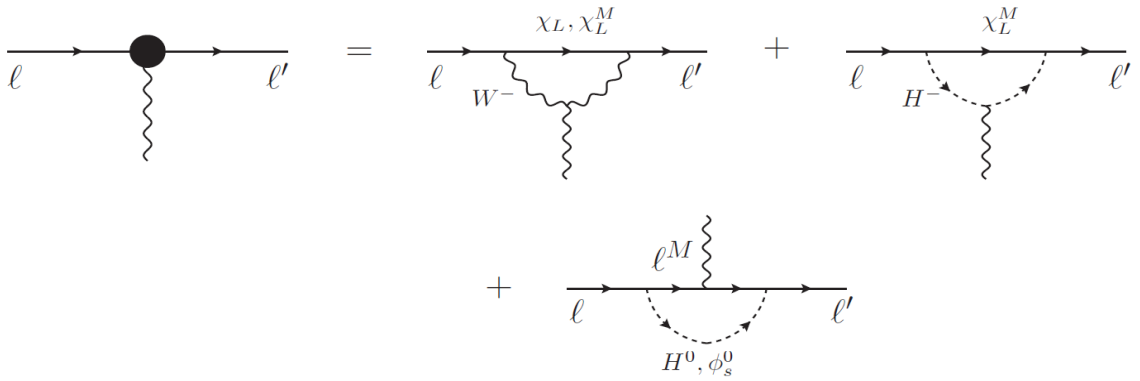

Fig. 1. Three groups of diagrams with photon exchange provide leading contributions to the $\mu - e$ conversion, where H^- stands for H_3^- and H_{3M}^-; H^0 stands for $\tilde{H}_i^0$, H_3^0 and H_{3M}^0.

$$(\bar{e}'_R e_L^{M\prime} \tilde{H}_i^0) \; -i\frac{g}{2} Y_{\tilde{H}_i^0}^{ML} = -i\frac{g}{2M_W}\left[\frac{\alpha_i}{s_2} m_\ell^d \tilde{R}_\ell + \frac{\alpha_i^M}{s_{2M}} \tilde{R}_\ell m_{\ell M}^d\right], \tag{15}$$

$$(\bar{e}'_L e_R^{M\prime} \tilde{H}_i^0) \; -i\frac{g}{2} Y_{\tilde{H}_i^0}^{MR} = -i\frac{g}{2M_W}\left[\frac{\alpha_i}{s_2} m_\ell^d \tilde{R}_\ell + \frac{\alpha_i^M}{s_{2M}} \tilde{R}_\ell m_{\ell M}^d\right], \tag{16}$$

$$(\bar{e}'_R e_L^{M\prime} H_3^0) \; -i\frac{g}{2} Y_{H_3^0}^{ML} = -i\frac{g}{2M_W}\left[\frac{s_M}{c_M} m_\ell^d \tilde{R}_\ell + \frac{s_M}{c_M} \tilde{R}_\ell m_{\ell M}^d\right], \tag{17}$$

$$(\bar{e}'_L e_R^{M\prime} H_3^0) \; -i\frac{g}{2} Y_{H_3^0}^{MR} = -i\frac{g}{2M_W}\left[-\frac{s_M}{c_M} m_\ell^d \tilde{R}_\ell - \frac{s_M}{c_M} \tilde{R}_\ell m_{\ell M}^d\right], \tag{18}$$

$$(\bar{e}'_R e_L^{M\prime} H_{3M}^0) \; -i\frac{g}{2} Y_{H_{3M}^0}^{ML} = -i\frac{g}{2M_W}\left[-\frac{s_{2M}}{s_2} m_\ell^d \tilde{R}_\ell - \frac{s_2}{s_{2M}} \tilde{R}_\ell m_{\ell M}^d\right], \tag{19}$$

$$(\bar{e}'_L e_R^{M\prime} H_{3M}^0) \; -i\frac{g}{2} Y_{H_{3M}^0}^{MR} = -i\frac{g}{2M_W}\left[\frac{s_{2M}}{s_2} m_\ell^d \tilde{R}_\ell + \frac{s_2}{s_{2M}} \tilde{R}_\ell m_{\ell M}^d\right]. \tag{20}$$

Here one has used the notations $U_{PMNS} = U_\ell^\dagger U_\nu$, which is the famous PMNS mixing matrix, $U_{PMNS}^M = U_\ell^{M\dagger} U_\nu^M$ and $\tilde{R}_{\ell(\nu)} = U_\ell^\dagger R_{\ell(\nu)} U_\ell^M$.

3. Phenomenology of $\mu - e$ conversion

3.1. One-loop form-factors and $\mu - e$ conversion ratio

To derive the $\mu - e$ conversion rate in a generic nucleus $\mathcal{N}$, one has to obtain the $\mu - e$ effective Lagrangian by calculating loop integral factors. In some previous works, one-loop diagrams with various kinds of internal lines have been detailedly calculated [12, 20–23]. In the current work, the leading effective charged lepton flavor-changing operators arise at one-loop level with photon exchange, where the virtual particles running inside are either physical Higgs scalars or W gauge bosons accompanied by relevant leptons. Their Feynman diagrams are shown in Fig. 1. The calculation result can be summarized as follows:

$$\begin{aligned}\mathscr{L}_{eff} &= -4\frac{eG_F}{\sqrt{2}}\left(m_\mu A_R\,\bar{e}\,\sigma^{\alpha\beta}P_R\,\mu\,F_{\beta\alpha}+m_\mu A_L\,\bar{e}\,\sigma^{\alpha\beta}P_L\,\mu\,F_{\beta\alpha}+\text{h.c.}\right)\\ &- \frac{e^2G_F}{\sqrt{2}}\left[\left(C_L^V\,\bar{e}\,\gamma^\alpha P_L\,\mu+C_R^V\,\bar{e}\,\gamma^\alpha P_R\,\mu\right)\sum_{Q=u,d}q_Q\overline{Q}\,\gamma_\alpha\,Q+\text{h.c.}\right].\end{aligned}\tag{21}$$

Here $A_{L,R}$, $C^V_{L,R}$ are the form factors:

$$\begin{aligned}A_R = &-\sum_{H^Q,k}\frac{M_W^2}{64\pi^2M_H^2}\left[\left(Y_H^L\right)_{\mu k}\left(Y_H^L\right)^*_{ek}G_H^Q(\lambda_k)+\frac{m_k}{m_\mu}\left(Y_H^R\right)_{\mu k}\left(Y_H^L\right)^*_{ek}\times R_H^Q(\lambda_k)\right]\\ &+\frac{1}{32\pi^2}\sum_k\left[\left(U^L\right)_{\mu k}\left(U^L\right)^*_{ek}G_\gamma(\lambda_k)-\frac{m_k}{m_\mu}\left(U^R\right)_{\mu k}\left(U^L\right)^*_{ek}R_\gamma(\lambda_k)\right],\end{aligned}\tag{22}$$

$$\begin{aligned}A_L = &-\sum_{H^Q,k}\frac{M_W^2}{64\pi^2M_H^2}\left[\left(Y_H^R\right)_{\mu k}\left(Y_H^R\right)^*_{ek}G_H^Q(\lambda_k)+\frac{m_k}{m_\mu}\left(Y_H^L\right)_{\mu k}\left(Y_H^R\right)^*_{ek}R_H^Q(\lambda_k)\right]\\ &+\frac{1}{32\pi^2}\sum_k\left[\left(U^R\right)_{\mu k}\left(U^R\right)^*_{ek}G_\gamma(\lambda_k)-\frac{m_k}{m_\mu}\left(U^L\right)_{\mu k}\left(U^R\right)^*_{ek}R_\gamma(\lambda_k)\right],\end{aligned}\tag{23}$$

$$C_L^V=-\sum_{H^Q,k}\frac{M_W^2}{8\pi^2M_H^2}\left(Y_H^L\right)_{\mu k}\left(Y_H^L\right)^*_{ek}V_H^Q(\lambda_k)+\frac{1}{4\pi^2}\sum_k\left(U^L_{W_\mu}\right)_{\mu k}\left(U^L_{W_\mu}\right)^*_{ek}V_\gamma(\lambda_k),\tag{24}$$

$$C_R^V=-\sum_{H^Q,k}\frac{M_W^2}{8\pi^2M_H^2}\left(Y_H^R\right)_{\mu k}\left(Y_H^R\right)^*_{ek}V_H^Q(\lambda_k)+\frac{1}{4\pi^2}\sum_k\left(U^R_{W_\mu}\right)_{\mu k}\left(U^R_{W_\mu}\right)^*_{ek}V_\gamma(\lambda_k),\tag{25}$$

where $H^Q=\phi_S^0,\tilde{H}_i^0$ $(i=1,2,3)$, H_3^0,H_{3M}^0, H_3^+,H_{3M}^+ is a particle with electric charge Q, and m_k are the masses of associated fermions that accompany with either H^Q or W_μ in the loops. Note that, the index k runs for all possible particles accompanying with H^Q, then the quantities $U^{L(R)}$, as an example for the case of gauge boson loop, can be $U^{L(R)}_{W_\mu}$ or $U^{ML(MR)}_{W_\mu}$ depending on the particle with index k whether the light or heavy neutrino, respectively. The same notations are used for $Y_H^{L(R)}$. The functions $G_H^Q(x)$, $R_H^Q(x)$, $G_\gamma(x)$, $R_\gamma(x)$, $V_\gamma(x)$ and $V_H^Q(x)$ listed from eqs. (22) to (25) are defined as:

$$G_H^Q(x) = -\frac{(3Q-1)x^2+5x-3Q+2}{12(x-1)^3}+\frac{1}{2}\frac{x(Qx-Q+1)}{2(x-1)^4}\log(x),\tag{26}$$

$$R_H^Q(x) = \frac{(2Q-1)x^2-4(Q-1)x+2Q-3}{2(x-1)^3}-\frac{Qx-(Q-1)}{(x-1)^3}\log(x),\tag{27}$$

$$V_H^Q(x) = \frac{(7-18Q)x^2+(36Q-29)x-18Q+16}{36(x-1)^3}+\frac{Qx^3-3(Q-1)x+2(Q-1)}{6(x-1)^4}\log(x),\tag{28}$$

$$G_\gamma(x) = \frac{11x^2-7x+2}{4(x-1)^3}-\frac{3}{2}\frac{x^3}{(x-1)^4}\log x,\ R_\gamma(x)=-\frac{x^2+x-8}{2(x-1)^2}+\frac{3x(x-2)}{(x-1)^3}\log(x),\tag{29}$$

$$V_\gamma(x) = -\frac{20x^2-33x+7}{12(x-1)^3}-\frac{x^4-10x^3+12x^2}{6(x-1)^4}\log(x),\tag{30}$$

where notation $\lambda_k=m_k^2/M^2_{W_\mu(H^Q)}$ has been used. Note that the functions $G_H^Q(x)$, $R_H^Q(x)$, $G_\gamma(x)$, $R_\gamma(x)$, $V_\gamma(x)$ and $V_H^Q(x)$, are valid for x variable varying in the interval $[0,+\infty)$.

Table 3. Nuclear parameters related to $\mu - e$ conversion in $^{48}_{22}$Ti, $^{27}_{13}$Al and $^{197}_{79}$Au are taken from [24].

$\mathcal{N}$	$D\, m_\mu^{-5/2}$	$V^{(p)}\, m_\mu^{-5/2}$	$V^{(n)}\, m_\mu^{-5/2}$	$\Gamma_{\rm capt}$ $(10^6\,{\rm s}^{-1})$
$^{48}_{22}$Ti	0.0864	0.0396	0.0468	2.590
$^{27}_{13}$Al	0.0362	0.0161	0.0173	0.7054
$^{197}_{79}$Au	0.189	0.0974	0.146	13.07

The expression for the $\mu - e$ conversion rate derived from effective Lagrangian (21) using the effective field theory approach developed in [24] arrives at

$$\begin{aligned} {\rm CR}(\mu\,\mathcal{N} \to e\,\mathcal{N}) \;\cong\; (4\pi\alpha_{\rm em})^2\,\frac{2\,G_F^2}{\Gamma_{\rm capt}} \Bigg(& \left| A_R\,\frac{D}{\sqrt{4\pi\,\alpha_{\rm em}}} + (2\,q_u + q_d)\,C_L^V\,V^{(p)} \right|^2 \\ & + \left| A_L\,\frac{D}{\sqrt{4\pi\,\alpha_{\rm em}}} + (2\,q_u + q_d)\,C_R^V\,V^{(p)} \right|^2 \Bigg). \end{aligned} \tag{31}$$

Here, $\alpha_{em} = 1/137$ is the fine-structure constant, G_F is the Fermi constant, and q_u and q_d are respectively the electric charges of quarks u and d. The quantities denoted by D and $V^{(p)}$ are overlap integrals of the muon and electron wave functions (see, *e.g.* [24]). Numerically, the parameters $D\,m_\mu^{-5/2}$, $V^{(p)}\,m_\mu^{-5/2}$, and $\Gamma_{\rm capt}$ for $^{48}_{22}$Ti, $^{27}_{13}$Al and $^{197}_{79}$Au are detailedly listed in Table 3.

3.2. The numerical analysis of $\mu - e$ conversion

In this section, we perform a numerical analysis of the $\mu - e$ conversion ratio expressed by (31) using the current and future expected experimental data. For better understanding and simplicity, we separately consider the contributions of one-loop diagrams with virtual W gauge boson, neutral and singly charged Higgs scalars. Moreover, we assume that three heavy neutrinos are degenerated in masses, which are denoted as m_χ^M. Similarly, the same assumption is supposed for three mirror charged lepton masses m_ℓ^M. Numerically, masses of heavy neutrinos, new charged leptons, and Higgs scalars (except ϕ_s^0) generated after the spontaneous symmetry breaking are expected to be in the range of the W mass to several hundreds GeV in the electroweak scale. Mass of the lightest physical scalar ϕ_s^0 is considered in the same range as v_S, which is supposed to be from hundreds of keV to a few tens of GeV.

The constraints on the magnitude of the interaction between W-boson and heavy neutrinos by the $\mu - e$ conversion in some given nuclei are intuitively shown in Fig. 2. The four peaks occurring in the figure can be understood as the vanishing of the first term in (31) at some specific values of the heavy neutrino mass, when the right sector does not participate in the process. The most stringent constraint to be obtained is: $\left| U_W^{ML\dagger} U_W^{ML} \right|_{e\mu}^2 \leq 7.02 \times 10^{-14}$, at $m_\chi^M = 80$ GeV, using

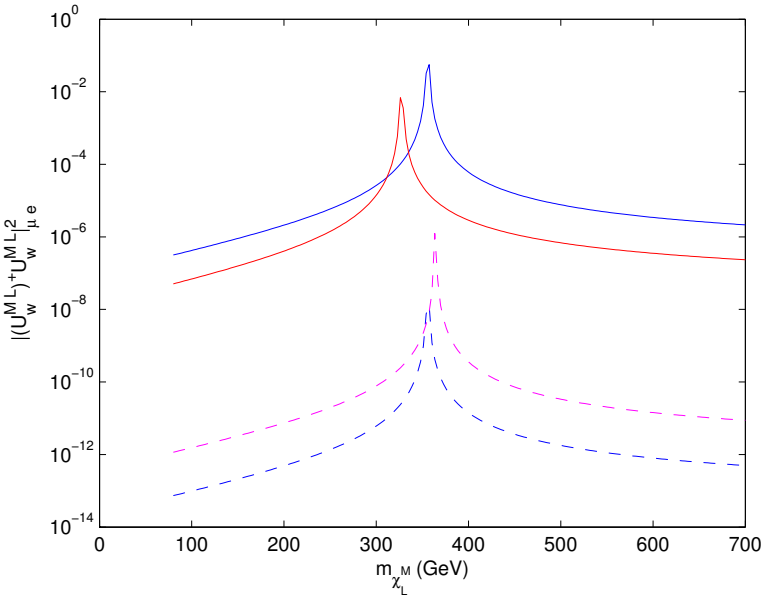

Fig. 2. The upper bound on $\left|U_W^{ML\dagger}U_W^{ML}\right|^2_{\mu e}$ as function of the heavy neutrino mass m_χ^M using: the current upper limit of $\mu - e$ conversion for nuclei i, $\mathrm{CR}(\mu\mathrm{Ti} \to e\mathrm{Ti}) < 4.3 \times 10^{-12}$ (solid blue); ii, $\mathrm{CR}(\mu\mathrm{Au} \to e\mathrm{Au}) < 7.0 \times 10^{-13}$ (solid red); and the future expected upper limit of $\mu - e$ conversion rate for nuclei iii, $\mathrm{CR}(\mu\mathrm{Al} \to e\mathrm{Al}) < 1.0 \times 10^{-17}$ (solid magenta); iv, and for $\mathrm{CR}(\mu\mathrm{Ti} \to e\mathrm{Ti}) < 10^{-18}$ (dash blue); for the channel of virtual W-boson and heavy neutrinos.

the future expected sensitivity of the $\mu - e$ conversion experiment for $^{48}_{22}$Ti. Upper bound of the above quantity, in fact, can be theoretically estimated in this model. Using the upper limit on light neutrino mass matrix, $\tilde{m}_\nu = \frac{(m_\nu^D)^2}{M_R} \sim 10^{-10}$ GeV and $R_\nu = \frac{m_\nu^D}{M_R} \sim 10^{-5}\sqrt{\frac{1\mathrm{GeV}}{M_R}}$, one easily implies $|R_\nu|^2 \sim 10^{-12}$ for $M_R \sim 100$ GeV. Therefore $\left|U_W^{ML\dagger}U_W^{ML}\right|^2_{e\mu} \sim |R_\nu|^4 \sim 10^{-24}$, which is about ten orders smaller then the upper bound obtained from the figure.

In contrast to the first case, in the later considered channels involving the neutral (both light and heavy) and singly charged Higgs scalars, both left and right sectors participate simultaneously. Therefore, their contributions to the conversion rate are substantially different. For these cases, it can be evaluated quantitatively from (22) and (23) that the dominated contributions are provided by the interference terms, which are enhanced by the factor $m_k/m_\mu \sim 1000$, where $m_\mu = 106$ MeV is the muon mass and $m_k \sim 100$ GeV is the heavy neutrino or mirror lepton mass, depending on the specific case. This fact is intuitively shown in Fig. 3 and Fig. 4 as an example for the cases of singly charged Higss scalars. Fig. 3 is produced when only Y_H^L is taken into account, while Fig. 4 is made when both Y_H^L and Y_H^R are considered. The constraints on the Yukawa couplings in Fig. 4 are much more stringent than those obtained from Fig. 3, which are consistent with the above estimation about the domination of the interference terms.

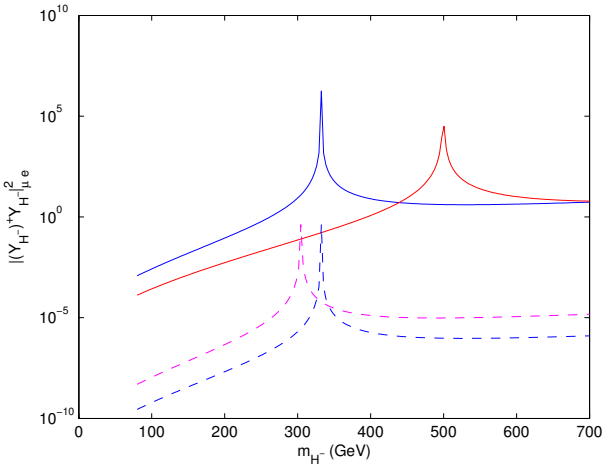

Fig. 3. Constraint on the relevant Yukawa couplings as function of scalar mass m_{H^-} for the case of singly charged Higgs scalar, when only Y_H^L is taken into account using: the current upper limit of $\mu - e$ conversion for nuclei i, $^{48}_{22}$Ti (solid blue); ii, $^{197}_{79}$Au (solid red); and the future expected upper limit of $\mu - e$ conversion rate for nuclei iii, $^{27}_{13}$Al (solid magenta); iv, and for $^{48}_{22}$Ti (dash blue).

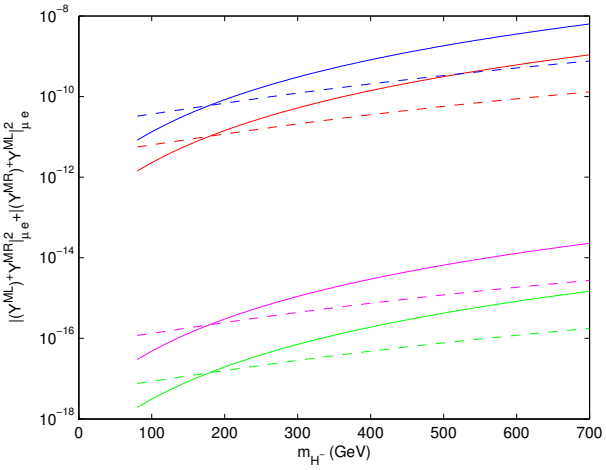

Fig. 4. Constraints by the $\mu - e$ conversion on the relevant Yukawa couplings for the case of singly charged Higgs scalar, when both Y_H^L and Y_H^R are taken into account. Here, $|(Y^{ML})^\dagger Y^{MR}|^2_{\mu e}+|(Y^{MR})^\dagger Y^{ML}|^2_{\mu e} = |(Y^{ML}_{H^-})^\dagger Y^{MR}_{H^-}|^2_{\mu e}+|(Y^{MR}_{H^-})^\dagger Y^{ML}_{H^-}|^2_{\mu e}$. The blue, red, magenta and green lines correspond respectively to the current upper limits of the $\mu - e$ conversion: i, $\mathrm{CR}(\mu\mathrm{Ti} \to e\mathrm{Ti}) < 4.3 \times 10^{-12}$; ii, $\mathrm{CR}(\mu\mathrm{Au} \to e\mathrm{Au}) < 7.0 \times 10^{-13}$, and to the future expected limits iii, $\mathrm{CR}(\mu\mathrm{Al} \to e\mathrm{Al}) < 1.0 \times 10^{-17}$; iv, $\mathrm{CR}(\mu\mathrm{Ti} \to e\mathrm{Ti}) < 10^{-18}$, for $m_\chi^M = 80$ (400) GeV, solid (dash) lines.

Fig. 4 shows curves with the shape of monotonically increasing functions, which implies that the stringency of the constraints on the Yukawa couplings reduces as the scalar mass m_{H^-} increases. At $m_{H^-} = 80$ GeV, for $m_\chi^M = 80$ GeV and using the current (or future expected) upper bounds on $\mu - e$ conversion ratios for nuclei $^{48}_{22}$Ti, one obtains respectively:

$$|(Y_{H^-}^{ML})^\dagger Y_{H^-}^{MR}|^2_{\mu e} + |(Y_{H^-}^{MR})^\dagger Y_{H^-}^{ML}|^2_{\mu e} \lesssim 8.23 \times 10^{-12} (1.90 \times 10^{-18}). \tag{32}$$

Note that the above equation is common for both H_3^- and H_{3M}^-. Direct calculation for the case of H_{3M}^- using Table 2, one has

$$\begin{aligned} \left|Y^{L\dagger}_{H^-_{3M}} Y^R_{H^-_{3M}}\right|^2_{21} \quad + \quad \left|Y^{R\dagger}_{H^-_{3M}} Y^L_{H^-_{3M}}\right|^2_{21} &= \left(\frac{s_M}{s_2 c_M^2}\right)^2 \frac{\left|m_\ell^d \tilde{R}_\nu m_{\ell M}^d \tilde{R}_\ell\right|^2_{21} + \left|\tilde{R}_\ell m_{\ell M}^d \tilde{R}_\nu m_\ell^d\right|^2_{21}}{M_W^4} \\ &\sim 10^{-24} \left(\frac{s_M}{s_2 c_M^2}\right)^2 \times \left(\frac{3 m_\mu m_\ell^M}{M_W^2}\right)^2 \sim 2.2 \times 10^{-29} \left(\frac{s_M}{s_2 c_M^2}\right)^2. \end{aligned} \tag{33}$$

To have (33), we have used $R_\ell \sim 10^{-6}$, which can be derived the same way as R_ν. While $\tilde{R}_{\ell(\nu)} = U_\ell^\dagger R_{\ell(\nu)} U_\ell^M \sim 10^{-6}$ are estimated to be at the same order as R_ℓ and R_ν, because the basis transformation matrices U_ℓ and U_ℓ^M are normalized. Additionally, the heavy neutrino and mirror lepton masses are assumed to be about 100 GeV. The upper limit in (33) still has distance with the upper bound given by the present best constraint on $\mu - e$ conversion for the $^{48}_{22}$Ti. However, it might be in the sensitivity range of the future experiment if s_2 and c_M are both not lager than about 0.01. For the case of H_3^-, the factor $(\frac{s_M}{s_2 c_M^2})^2$ is replaced by $(\frac{s_M}{c_M^2})^2$, that makes (33) harder to be within the sensitive limit of about 10^{-18}, which satisfies only for $c_M < 0.001$. However, these cases are not realistic, because, for example, if s_2 is small, which leads to a small magnitude of v_2, then it cannot provide accurate masses for the heavy quarks.

Finally, the constraints on the relevant Yukawa couplings as functions of the neutral heavy (light) scalar masses are shown in the Figure 5, in the left (right) panel, respectively. The upper bounds for the cases of the heavy neutral scalars using the current (near future) experiments with $^{48}_{22}$Ti, for $m_\ell^M = 80$ GeV and $m_{H^0} = 80$ GeV, read:

$$|(Y_{H^0}^{ML})^\dagger Y_{H^0}^{MR}|^2_{\mu e} \lesssim 1.06 \times 10^{-12} (2.29 \times 10^{-18}). \tag{34}$$

To evaluate the sensitivity of the under consideration channel with the experiments, let's compare (34) with the theoretical estimation of $|(Y_{H^0}^{ML})^\dagger Y_{H^0}^{MR}|^2_{\mu e}$, which is

$$\left|Y^{L\dagger}_{H^0} Y^R_{H^0}\right|^2_{21} = \alpha^4 \times \frac{\left|\tilde{R}_\ell (m_{\ell M}^d)^2 \tilde{R}_\ell\right|^2_{21}}{M_W^4} \sim 2.2 \times 10^{-23} \alpha^4, \tag{35}$$

where α stands for $\frac{\alpha_i}{s_2}$, $\frac{s_M}{c_M}$ or $\frac{s_2}{s_{2M}}$, corresponding to $\tilde{H}_i^0$, $(i = 1,2,3)$, H_3^0 or H_{3M}^0, respectively. Compare with the previous case (see (33)), this result is about six orders more sensitive. For instance, if $c_M = 0.01$, one easily has $\left|Y^{L\dagger}_{H^0_{3M}} Y^R_{H^0_{3M}}\right|^2_{21} \sim 2.2 \times 10^{-15}$, which is about three times larger than the required value to be within the sensitivity of the future experiment. In fact, to reach the future sensitive limit given in (34), the appropriate c_M is not larger than 0.056. Similar results are also obtained for other heavy neutral scalars, $\tilde{H}_i^0$, $(i = 1,2,3)$ and H_3^0.

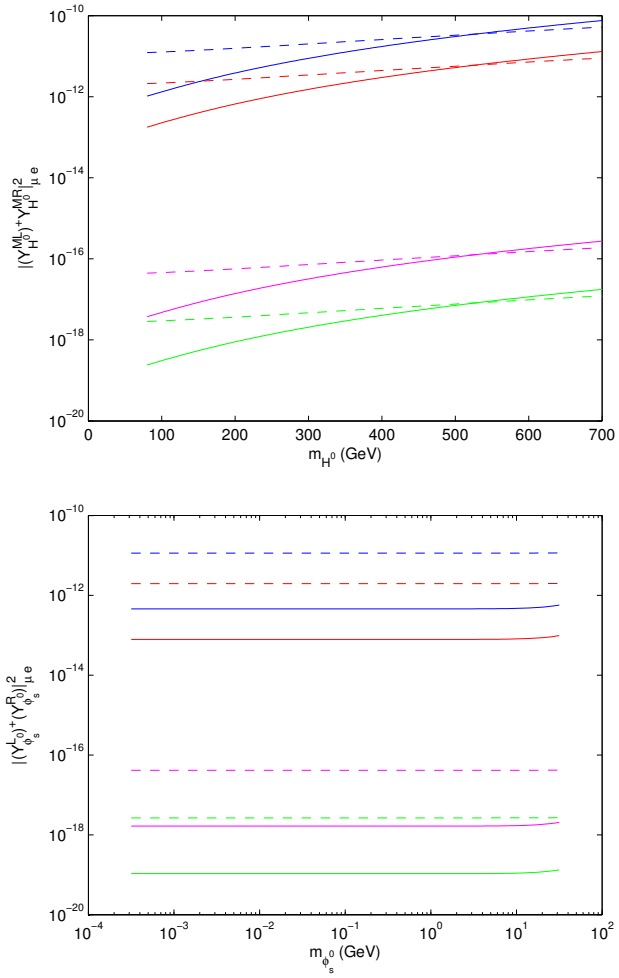

Fig. 5. Upper constraints on the Yukawa couplings as functions of the mass of the neutral heavy (light) scalar, shown in the top-panel (bottom-panel) for $m_\ell^M = 80\ (400)$ GeV as solid (dash) lines. The blue, red, magenta and green lines correspond respectively to the current upper limits of the $\mu - e$ conversion for nuclei $^{48}_{22}$Ti, $^{197}_{79}$Au, and to the future expected limits for $^{27}_{13}$Al and $^{48}_{22}$Ti.

For the channel of the light neutral scalar, constraints on the Yukawa couplings are shown in the left-panel of Figure 5. The figure shows that lines describing the constrained stringency are constantly depended on the light neutral Higgs mass until about 10 GeV, then slowly go up. In the steady region, one has for the cases of $^{48}_{22}$Ti nuclei that

$$|(Y^L_{\phi^0_s})^\dagger Y^R_{\phi^0_s}|^2_{\mu e} \lesssim 4.46 \times 10^{-13} (1.06 \times 10^{-18}). \tag{36}$$

This result can be recasted as

$$|\tilde{g}^\dagger_{\ell s} \tilde{g}_{\ell s}|_{\mu e} \leq 5.29 \times 10^{-8} (7.92 \times 10^{-11}). \tag{37}$$

Note that (36) and (37) are derived respectively using the current (future) experimental sensitivities and at $m_\ell^M = 80$ GeV. In fact, the upper bounds on the magnitude of $|g_{\ell s}|$ have been specified in some previous phenomenological researches. For instant, by studying the decay $H_3^0 \to \bar{\ell}^M \ell^M \to \bar{\ell}\phi_s \ell \phi_s^*$, where ϕ_s is invisible and considered as missing transverse energy, due to no excess over the background was detected at both ATLAS and CMS, one has an upper limit $|g_{\ell s}|^2 \leq 10^{-6}$ (see [7]). Less stringent than the above, the constraint from the anomaly of muon magnetic dipole moment implies $|\tilde{g}^\dagger_{\ell s}\tilde{g}_{\ell s}|_{\mu\mu} \simeq 5.39 \times 10^{-5}$ [13]. Moreover, using the current (expected future) sensitivities of the lepton flavor violation decay $\mu \to e\gamma$, the result $|\tilde{g}^\dagger_{\ell s}\tilde{g}_{\ell s}|_{\mu e} \leq 5.29 \times 10^{-10}$ (1.96×10^{-10}) for $m_\ell^M = 80$ GeV is obtained in [12]. The current constraint by $\mu \to e\gamma$ decay is indeed more stringent then that given by the present upper bound on $\mu - e$ conversion. However, the future planned experiment of $\mu - e$ conversion is more sensitive than the $\mu \to e\gamma$ decay in the framework of the under consideration model.

4. Conclusion

In this research, we have briefly introduced the model of low energy scale type I see-saw with mirror symmetry, and performed numerical analysis for the $\mu - e$ conversion using the current and future experimental sensitivities. The conversion rate is calculated at one-loop approximation with participation of neutrinos along with W boson or singly charged scalars and light or heavy neutral scalars with charged leptons. The contributions of channels with neutrinos and singly charged scalars are insignificant and can be disregarded. While the contributions of the both light and heavy neutral scalar channels are shown to be able to reach the sensitivity of the designed experiment of the $\mu - e$ conversion for $^{48}_{22}$Ti nuclei. Much more sensitive than the cases of singly charged ones, the channels of light and heavy neutral scalars have less stringent constraints on the Yukawa couplings for the conversion signals to be probed by the future experiment. For instance, for the case of H_{3M}^0, the couplings might reach the sensitive limit with $c_M \leq 0.056$. As the most promising case, the contribution of light scalar channel also has potential to be within the future experimental sensitive range for $|\tilde{g}^\dagger_{\ell s}\tilde{g}_{\ell s}|_{\mu e} > 7.92 \times 10^{-11}$. Moreover, in the framework of this model, the planned $\mu - e$ conversion experiment is demonstrated to be more sensitive than the future $\mu \to e\gamma$ decay experiment.

Acknowledgments

This research is funded by Vietnam National Foundation for Science and Technology Development (NAFOSTED) under grant number 103.01-2019.307.

References

[1] P. Q. Hung, *A Model of electroweak-scale right-handed neutrino mass*, Phys. Lett. B **649** (2007) 275.
[2] P. Minkowski, $\mu \to e\gamma$ *at a Rate of One Out of* 10^9 *Muon Decays?*, Phys. Lett. B **67** (1977) 421.
[3] M. Gell-Mann, P. Ramond and R. Slansky, *Complex Spinors and Unified Theories*, Conf. Proc. C **790927** (1979) 315.
[4] T. Yanagida, *Horizontal gauge symmetry and masses of neutrinos*, Conf. Proc. C **7902131** (1979) 95.
[5] R. N. Mohapatra and G. Senjanovic, *Neutrino Masses and Mixings in Gauge Models with Spontaneous Parity Violation*, Phys. Rev. D **23** (1981) 165.
[6] P. Q. Hung, T. Le, V. Q. Tran and T.-C. Yuan, *Lepton Flavor Violating Radiative Decays in EW-Scale* ν_R *Model: An Update*, JHEP **12** (2015) 169.

[7] V. Hoang, P. Q. Hung and A. S. Kamat, *Non-sterile electroweak-scale right-handed neutrinos and the dual nature of the 125-GeV scalar*, Nucl. Phys. B **896** (2015) 611.
[8] V. Hoang, P. Q. Hung and A. S. Kamat, *Electroweak precision constraints on the electroweak-scale right-handed neutrino model*, Nucl. Phys. B **877** (2013) 190.
[9] P. Q. Hung, *Electroweak-scale mirror fermions, mu —> e gamma and tau —> mu gamma*, Phys. Lett. B **659** (2008) 585.
[10] C.-F. Chang, P. Q. Hung, C. S. Nugroho, V. Q. Tran and T.-C. Yuan, *Electron Electric Dipole Moment in Mirror Fermion Model with Electroweak Scale Non-sterile Right-handed Neutrinos*, Nucl. Phys. B **928** (2018) 21.
[11] P. Q. Hung, T. Le, V. Q. Tran and T.-C. Yuan, *Muon-to-Electron Conversion in Mirror Fermion Model with Electroweak Scale Non-Sterile Right-handed Neutrinos*, Nucl. Phys. B **932** (2018) 471 [1701.01761].
[12] D. N. Dinh, *The $\mu \to e\gamma$ decay in an EW-scale non-sterile RH neutrino model*, Eur. Phys. J. C **82** (2022) 295.
[13] D. N. Dinh, *Muon anomalous magnetic dipole moment in a low scale type I see-saw model*, Nucl. Phys. B **994** (2023) 116306.
[14] SINDRUM II collaboration, *Test of lepton flavor conservation in mu —> e conversion on titanium*, Phys. Lett. B **317** (1993) 631.
[15] SINDRUM II collaboration, *A Search for muon to electron conversion in muonic gold*, Eur. Phys. J. C **47** (2006) 337.
[16] R. J. Barlow, *The PRISM/PRIME project*, Nucl. Phys. B Proc. Suppl. **218** (2011) 44.
[17] MU2E collaboration, *Mu2e Technical Design Report*, 1501.05241.
[18] COMET collaboration, *COMET Phase-I Technical Design Report*, PTEP **2020** (2020) 033C01.
[19] M. S. Chanowitz and M. Golden, *Higgs Boson Triplets With M (W) = M (Z) $\cos\theta\omega$*, Phys. Lett. B **165** (1985) 105.
[20] R. Alonso, M. Dhen, M. B. Gavela and T. Hambye, *Muon conversion to electron in nuclei in type-I seesaw models*, JHEP **01** (2013) 118 [1209.2679].
[21] A. G. Akeroyd, M. Aoki and H. Sugiyama, *Lepton Flavour Violating Decays tau —> anti-l ll and mu —> e gamma in the Higgs Triplet Model*, Phys. Rev. D **79** (2009) 113010.
[22] D. N. Dinh, A. Ibarra, E. Molinaro and S. T. Petcov, *The $\mu - e$ Conversion in Nuclei, $\mu \to e\gamma, \mu \to 3e$ Decays and TeV Scale See-Saw Scenarios of Neutrino Mass Generation*, JHEP **08** (2012) 125.
[23] D. N. Dinh, D. T. Huong, N. T. Duy, N. T. Nhuan, L. D. Thien and P. Van Dong, *Flavor changing in the flipped trinification*, Phys. Rev. D **99** (2019) 055005.
[24] R. Kitano, M. Koike and Y. Okada, *Detailed calculation of lepton flavor violating muon electron conversion rate for various nuclei*, Phys. Rev. D **66** (2002) 096002.